SLAC-PUB-7200
June 1996

Preliminary Measurement of D^*/D Production and D^* Spin Alignment at the Z^0 Resonance*

The SLD Collaboration**
Stanford Linear Accelerator Center
Stanford University, Stanford, CA 94309

*This work was supported by Department of Energy contracts: DE-FG02-91ER40676 (BU), DE FG03-91ER40618 (UCSB), DE-FG03-92ER40689 (UCSC), DE-FG03-93ER40788 (CSU), DE-FG02-91ER40672 (Colorado), DE-FG02-91ER40677 (Illinois), DBAC03-76SF00098 (LBL), DE-FG02-92ER40715 (Massachusetts), DE-AC02-76ER03069 (MIT), DE-FG06-85ER40224 (Oregon), DEAC03-76SF00515 (SLAC), DE-FG05-91ER40627 (Tennessee), DEFG02-95ER40896 (Wisconsin), DEFG02-92ER40704 (Yale); National Science Foundation grants: PHY-91-13428 (UCSC), PHY-89-21320 (Columbia), PHY-92-04239 (Cincinnati), PHY-88-17930 (Rutgers), PHY-88-19316 (Vanderbilt), PHY-92-03212 (Washington); the UK Science and Engineering Research Council (Brunel and RAL); the Istituto Nazionale di Fisica Nucleare of Italy (Bologna, Ferrara, Frascati, Pisa, Padova, Perugia); and the Japan-US Cooperative Research Project on High Energy Physics (Nagoya, Tohoku).

Ref: PA04-046
Submitted to the 28th International Conference on High Energy Physics, Warsaw, Poland, July 25-31, 1996

ABSTRACT

Using hadronic Z^0 decays recorded by the SLD experiment at SLAC, we have measured the vector/(vector+pseudoscalar) production ratio, $V/(V+P)$, for the prompt charmed mesons, D^{*+} and D^+. Using the channels $D^{*+} \to D^0 \pi_s^+$, $D^0 \to K^- \pi^+$, and $D^0 \to K^- \pi^+ \pi^- \pi^+$, as well as $D^+ \to K^- \pi^+ \pi^-$, we find $V/(V+P) = 0.57 \pm 0.07(stat.) \pm 0.02(BR)$, which disfavors the expectation of 0.75 from naive spin-counting. We have also measured the degree of D^{*+} spin alignment along the flight direction and find it to be consistent with zero for D^{*+} fractional momenta $x \equiv ED. /E_{beam} > 0.2$. We compare these results with QCD model predictions.

1 Introduction

The fragmentation of heavy quarks has been studied both theoretically and experimentally. Some of the theoretical models are quite successful in describing experimental data collected in e^+e^- annihilation. Spin dependent properties of the fragmentation, such as the relative vector to pseudoscalar meson production ratio or the spin alignment of a vector meson, may be useful in studying the dynamics.

The ratio, P_V , which is defined as the relative production ratio of vector(V) to (vector+pseudoscalar(P)) mesons, is expected to be $V/(V+P) = 0.75$ using a naive spin-counting model. For charmed mesons recent measurements from LEP have yielded values lower then the naive expectation, $P_V = 0.53 \pm 0.16$ (ALEPH) [1] and 0.54 ± 0.10 (DELPHI) [2]. Other models for P_V , based on perturbative QCD, by Suzuki [3] and by Braaten, Cheung, and Yuan [4], predict a dependence on the fractional energy carried by the vector meson, $x_D = 2E/\sqrt{s}$, where $\sqrt{s}$ is the c.m. energy.

The degree of vector meson spin alignment along the flight direction is another aspect of spin-dependent effects in the fragment at ion process. The degree of vector meson spin alignment along the flight direction, α, is expected to be zero in the naive spin-counting model. Suzuki and Braaten, Cheung, and Yuan, have calculated α and found that it depends on x_D [3, 4].

Here we present the preliminary results of a study of the production of charmed vector and pseudoscalar mesons in Z^0 decay events produced by the SLAC Linear Collider (SLC) and recorded by the SLC Large Detector (SLD) experiment. By comparing the number of D^{*+} and D^+ mesons found*, we measured P_V as a function of x_D. We also measured the degree of D^{*+} spin alignment and its dependence on x_D. This represents the first study of D^{*+} spin alignment in Z^0 decays. We compared our results with those from lower energy experiments, as well as with the predictions of the spin-counting model and the models of Suzuki and of Braaten, Cheung, and Yuan.

*Charge-conjugate are implied unless stated otherwise.

2 Apparatus and Hadronic Event Selection

The e^+e^- annihilation events produced at the Z^0 resonance by the SLAC Linear Collider (SLC) have been recorded using the SLC Large Detector (SLD). A general description of the SLD can be found elsewhere [5]. Charged tracks are measured in the central drift chamber (CDC) [6] and in the vertex detector (VXD) [7]. Momentum measurement is provided by a uniform axial magnetic field of 0.6 T. The VXD is composed of CCDs containing a total of 120 million 22 $\times 22\mu m^2$ pixels arranged in four concentric layers of radius between 2.9 and 4.2 cm. Including the uncertainty on the primary interaction point (IP), the CDC and VXD give a combined impact parameter resolution of 11 $\oplus 76/(p_T\sqrt{sin\theta})\mu$m, where p_T is the track momentum transverse to the beam axis in GeV/c and θ is the track polar angle with respect to the beamline. Particle energies are measured in the Liquid Argon Calorimeter (LAC) [8], which contains both electro-magnetic and hadronic sections, and in the Warm Iron Calorimeter [9].

Three triggers were used for hadronic events. The first required a total LAC electromagnetic energy greater than 12 GeV; the second required at least two well-separated tracks in the CDC; and the third required at least 4 GeV in the LAC and one track in the CDC. The selection of hadronic events is described in [10].

The analysis presented here used the charged tracks measured in the CDC and VXD. A set of cuts was applied to the data to select well-measured tracks and events well-contained within the detector acceptance. Charged tracks were required to have (i) a closest approach transverse to the beam axis within 5 cm, and within 10 cm along the axis from the measured interaction point; (ii) a polar angle θ with respect to the beam axis within $|\cos\theta| < 0.80$; and (iii) a momentum transverse to the beam axis, $p_\perp > 0.15$ GeV/c. Events were required to have (i) a minimum of five such tracks; (ii) a thrust axis [11] direction within $|\cos\theta_T| < 0.71$; and (iii) a total visible energy E_{vis} of at least 20 GeV, which was calculated from the selected tracks assigned the charged pion mass. From our 1993-95 data sample 102,564 events passed these cuts. The efficiency for selecting hadronic events satisfying the $|\cos\theta_T|$ cut was estimated to be above 96%. The background in the selected event sample was estimated to be $0.3 \pm 0.1\%$, dominated by $Z^0 \to \tau^+\tau^-$ events. Distributions of single particle and event topology observable in the selected events were found to be well described by Monte Carlo models of hadronic Z^0 decays [12, 13] combined with a simulation of the SLD.

3 D^{*+} and D^+ selection

D^{*+} and D^+ mesons can be produced in $Z^0 \to c\bar{c}$ events, as well as from B hadron decays in $Z^0 \to b\bar{b}$ events. We describe the first category as primary mesons, and the second as secondary mesons. In order to measure the number of primary D mesons, we first reconstructed D meson candidates in various decay modes and applied cuts to reduce random combinatorics background (RCBG). We then divided the candidates between "c-rich" and "b-rich" samples using their impact parameters and proper decay times, as well as information from the opposite hemisphere of the events. Numbers of D mesons extracted from these two samples were then unfolded to yield the primary production rates in a manner independent of B hadron decay modeling.

The D^{*+} mesons were identified using the decay $D^{*+} \to D^0\pi_s^+$ followed by $D^0 \to K^-\pi^+$ ($K\pi$ mode) or $D^0 \to K^-\pi^+\pi^-\pi^+$ ($K\pi\pi\pi$ mode). The π_s^+ in the D^{*+} decay is known as the spectator pion. The D^{*+} sample is discriminated effectively from random combinatorics background (RCBG) by examining the mass difference between the D^{*+} and D^0 candidates. The selection criteria for the $K\pi$ and $K\pi\pi\pi$ modes are slightly different due to the different track multiplicities.

We first searched for D^0 candidates via the $K\pi$ and $K\pi\pi\pi$ decay modes. Each event was divided into two hemispheres by the plane perpendicular to the thrust axis. In each hemisphere we considered two ($K\pi$) or four ($K\pi\pi\pi$) track combinations whose net charge was zero, and assigned the K mass to one of the particles and the π mass to the other(s). For the $K\pi\pi\pi$ mode all tracks were required to have $p > 0.75\ GeV/c$. If the D^0 candidate mass lies in the range 1.765 $GeV/c^2 < M_{K\pi} <$ 1.965 GeV/c^2 or

$1.795 GeV/c^2 < M_{K\pi\pi\pi} < 1.935\ GeV/c^2$, it was combined with a π_s candidate track having charge opposite to the *K* candidate to form a D^{*+} candidate.

Candidates for $D^+ \rightarrow K^- \pi^+ \pi^-$ were formed by combining two same-sign pion candidates with an opposite-sign kaon candidate in one hemisphere. We required (i) $x_{D^+} > 0.2$, where $x_{D^+} = 2E_{D^+}/\sqrt{s}$, (ii) $cos\theta_K^+ > -0.8$, where θ_K^+ is the opening angle between the direction of the D^+ in the lab frame and the *K* in the D^+ rest frame, (iii) all three tracks to have $p > 1\ GeV/c$. To reject D^{*+} decays, the differences between $M_{K^-\pi^+\pi^+}$ and $M_{K^-\pi^+}$ were formed for each pion candidate, and both were required to be greater than 0.160 GeV/c^2.

To divide the sample into c-rich and b-rich subsamples we first applied an impact parameter technique [14] to hemispheres opposite to those containing a D meson candidate. We counted the number of significant tracks, N_{sig}, with normalized transverse impact parameter with respect to the interaction point $b/\sigma_b > 3$. Candidates with $N_{sig} \geq 3$ were assigned to the b-rich sample.

The candidates with $N_{sig} < 3$ were subjected to a decay length analysis. The tracks forming the D^0 or D^+ candidate were fitted to a common vertex and the decay length, *L*, was defined to be the distance in 3D from the IP to the fitted vertex position. The proper decay time is defined as $\tau = L/\gamma\beta c$. In order to suppress RCBG we use the fact that D^0 in $c\bar{c}$ as well as $b\bar{b}$ events have a long decay length, $\langle L \rangle \sim$ 1mm for the primary mesons and longer for the secondary mesons. Since the decay length resolution is $\langle \sigma_L \rangle \sim 200\ \mu$m, clean separation of these events from RCBG is possible. We required (i) a decay length significance $L/\sigma_L > 2.5$ for D^0 and $L/\sigma_L > 3.0$ for D^+, (ii) χ^2 probability > 1% for the vertex fit, and (iii) $x_{D^*} > 0.2$ $(K\pi)$ or 0.4 $(K\pi\pi\pi)$ for D^{*+}, (iv) the projection of the angle, ϕ, between the D^+ momentum vector and the vertex flight direction to be less than 15 mrad in the xy plane and 20 mrad in the rz plane for D^+. To separate primary from secondary D mesons we used the fact that D^0 in $c\bar{c}$ events are produced at the Z^0 primary vertex but in $b\bar{b}$ events at the B decay point. For the c-rich D^{*+} sample we required $d_{xy} < 20\mu$m, where d_{xy} is the *xy*

x_D	$D^{*+} \to \pi_s^+(K^-\pi^+)$		$D^{*+} \to \pi_s^+(K^-\pi^+\pi^-\pi^+)$		$D^+ \to K^-\pi^+\pi^-$	
	c-rich	b-rich	c-rich	b-rich	c-rich	b-rich
0.2-0.4	18.0/12.0	34.5/33.5	–	–	32.5/140.5	16.4/279.6
0.4-0.5	34.4/24.6	24.2/5.8	11.8/25.2	21.8/30.2	42.8/ 48.2	3.6/ 74.4
0.5-0.6	28.3/9.7	5.6/2.4	38.3/73.7	14.4/12.6	30.9/ 49.1	8.2/ 36.8
0.6-0.7	22.5/4.5	3.9/1.1	29.5/26.5	4.7/ 2.3	41.9/ 17.1	2.3/ 13.7
0.7-0.9	22.4/2.6	3.0/0.0	18.3/ 9.7	10.1/ 0.9	51.1/ 10.9	14.1/ 1.9

Table 1: Numbers of signal/background events in c-rich and b-rich samples for each D decay mode.

impact parameter of the D^0 momentum w.r.t. the interaction point, and $\tau_{D^0} < 1.0$ps, with the remaining candidates assigned to the b-rich sample. The D^+ candidates with $\phi_{xy} < 5$ mrad were assigned to the c-rich sample and the rest to the b-rich sample. At high momentum there are relatively few secondaries and so D^{*+} candidates were also accepted into the c-rich sample if the passed a set of kinematic cuts. We required (i) $x_{D^*} > 0.4$ $(K\pi)$ or 0.5 $(K\pi\pi\pi)$, where $x_{D^*} = 2E_{D*}/\sqrt{s}$, (ii) $|cos\theta_K^0| < 0.9$ $(K\pi)$ or 0.8 $(K\pi\pi\pi)$, where θ_K^0 is the angle between the direction of the D^0 in the lab frame and the K in the D^0 rest frame, and (iii) $p_{\pi_s} > 1GeV/c$. RCBG was reduced in the b-rich D^{*+} sample by requiring candidates to pass either these kinematic cuts or the decay length cuts (i)-(iii) above.

The mass difference, Δm, between the D^{*+} and D^0 was formed if an event satisfied the D^{*+} selection criteria. The Δm distribution for the combined c-rich and b-rich samples for the $K\pi(K\pi\pi\pi)$ mode is shown in Figure 1a (1b). The mass distribution of $D^+ \to K^-\pi^+\pi^-$ candidates, is also shown in Figure 1c. The number of signal D^{*+} in each of four x_{D^*} slices of each of the c-rich and b-rich samples was extracted from the Δm distribution, by fitting a Gaussian signal plus a background of the from $A(\Delta m - m_\pi)^B$. Results are shown in table 1 for signal and background integrated over

x_D	$D^{*+} \to \pi_s^+(K^-\pi^+)$		$D^{*+} \to \pi_s^+(K^-\pi^+\pi^-\pi^+)$		$D^+ \to K^-\pi^+\pi^-$	
	$N_{c\to D^{*+}}$	$N_{b\to D^{*+}}$	$N_{c\to D^{*+}}$	$N_{b\to D^{*+}}$	$N_{c\to D^+}$	$N_{b\to D^+}$
0.2-0.4	47.2±29.9	182.9±54.0	–	–	177.7±149.9	374.7±457.2
0.4-0.5	47.7±21.3	83.7±24.6	16.7±47.9	157.2±62.3	212.7± 65.1	−77.3±153.3
0.5-0.6	54.1±15.7	5.9±17.3	83.9±33.2	61.6±36.3	98.6± 62.2	82.1±140.0
0.6-0.7	39.7±11.7	2.8±15.5	87.5±26.4	−1.6±31.9	155.7± 34.7	−64.3± 83.9
0.7-0.9	47.7±14.4	1.7±28.2	30.3±18.9	40.0±22.0	120.3± 37.8	89.1± 76.0

Table 2: Extracted flavor-unfolded events in $c\bar{c}$ and $b\bar{b}$ events for each D decay mode. Errors are statistical only.

the range 0.142 < Δm < 0.149 GeV/c^2. Similarly, a Gaussian signal plus a third order polynomial function for the background was fitted to the mass distributions of the D^+ candidates, and results for range 1.800 < $M_{K\pi\pi} < 1.940 GeV/c^2$ are shown in Table 1.

For either the D^{*+} or D^+ mesons, the numbers of signal events in the c-rich and b-rich samples, N_{c-rich} and N_{b-rich} respectively, are related to the number of actual D mesons in $c\bar{c}$ events ($N_{c\to D}$) and in $b\bar{b}$ events ($N_{b\to D}$) as follows:

$$\begin{pmatrix} N_{c-rich} \\ N_{b-rich} \end{pmatrix} = \begin{pmatrix} \epsilon_c & \epsilon_b \\ \eta_c & \eta_b \end{pmatrix} \begin{pmatrix} N_{c\to D} \\ N_{b\to D} \end{pmatrix} . \qquad (1)$$

The tagging efficiencies, $\epsilon_{c,b}, \eta_{c,b}$, were estimated from the Monte Carlo simulation, and the matrix equation was solved for $N_{c\to D}$ and $N_{b\to D}$ to extract the measured numbers of D^{*+} and D^+ mesons in $c\bar{c}$ and $b\bar{b}$ events. These are shown in Table 2 with statistical errors.

4 Measurement of P_V

The measured numbers of D^{*+} and D^+ mesons in $c\bar{c}$ events, $N_{c\to D^{*+}}$ and $N_{c\to D^+}$ respectively, are related to the quantity P_V via:

$$\frac{N_{c\to D^{*+}}}{N_{c\to D^+}} \cdot \frac{Br_+}{Br_0} = \frac{P_V Br_*}{1 - P_V Br_*}, \quad (2)$$

where Br_* = 68.1 $\pm$ 1.0 $\pm$ 1.3% *[15]* is the branching fraction for $D^{*+} \to D^0 \pi_s^+$, Br_0 = 3.84 $\pm$ 0.13%, 7.50 $\pm$ 0.4% and Br_+ = 9.1 $\pm$ 0.6% [16] are the branching fractions for $D^0 \to K^-\pi^+$, $D^0 \to K^-\pi^+\pi^-\pi^+$, and $D^+ \to K^-\pi^+\pi^-$. We considered separately the number of D^{*+} formed from each D^0 decay mode and solved equation (2) in each bin of x_D. We obtained results for P_V shown in Table 3 and Figure 2, where the branching fraction errors have been added in quadrature to the statistical errors.

x_D	P_V	
	$D^{*+} \to \pi_s^+(K^-\pi^+)$	$D^{*+} \to \pi_s^+(K^-\pi^+\pi^-\pi^+)$
0.2-0.4	0.57±0.37	–
0.4-0.5	0.51±0.18	0.13±0.34
0.5-0.6	0.83±0.25	0.75±0.28
0.6-0.7	0.55±0.13	0.60±0.14
0.7-0.9	0.71±0.16	0.34±0.19
0.4-1.0	0.63±0.08	0.46±0.09

Table 3: P_V as a function of x_D for $K\pi$ and $K\pi\pi\pi$ modes. Statistical and branching fraction errors are combined for the errors of P_V.

Averaging over the region $x_D > 0.4$, we obtain P_V = 0.629 $\pm$ 0.084 for the $K\pi$ mode and P_V = 0.464 $\pm$ 0.092 for the $K\pi\pi\pi$ mode, where the errors are the sum in quadrature of the statistical errors and the branching fraction errors. The results are consistent within the errors so we averaged them to obtain P_V = 0.53 $\pm$ 0.06(*stat.*) $\pm$

0.02 (BR) (PRELIMINARY). This result is not consistent with the naive spin-counting expectation of P_V =0.75, but is in agreement with previous measurements from LEP experiments [1] [2]. These results can also be compared with QCD calculations. P_V as a function of x_D is shown in Figure 2, together with the predictions of Braaten, Cheung and Yuan and Suzuki. The predictions are consistent with the data within errors.

5 Measurement of D^{*+} spin alignment

We measured the degree of D^{*+} spin alignment along the flight direction by considering the angle θ^* between the momentum direction of the D^{*+} in the laboratory frame and the D^0 in the D^{*+} rest frame. In order to avoid a kinematic bias to the angular distribution of θ^*, we used only D^{*+} candidates passing the decay length cuts listed above. The distributions of $cos\theta^*$ for D^{*+} candidates with 0.142 < Δm < 0.149 GeV/c^2 in the combined c-rich and b-rich samples are shown in Figure 3 for four x_{D^*} bins, after statistical subtraction of the RCBG. The RCBG contribution was estimated using the Monte Carlo events normalized by the numbers of background events in the signal region of data. We then fitted the function:

$$\frac{1}{N}\frac{dN}{dcos\theta^*} = \frac{3}{(6+2\alpha)}[1+\alpha cos^2\theta^*], \qquad (3)$$

to each distribution. The parameter α quantifies the degree of spin alignment and a priori can have any value in the range $-1 \geq \alpha \geq \infty$. For $\alpha = -1$, the decay-angular distribution is proportional to $sin^2\theta$ and for $\alpha \rightarrow \infty$ the distribution is proportional to $cos^2\theta$. The fitted α, for each x_{D^*} bin, are listed in Table 4 and shown in Figure 4.

These results are consistent with previous measurements from CLEO [17], HRS [18], and TPC [19] at lower *c.m.* energy. QCD calculations by Suzuki and, by Braaten, Cheung and Yuan are also shown in Figure 4. Suzuki's calculation is disfavored by the data.

x_{D^*}	α
0.30	-0.16 ± 0.57
0.44	0.26 ± 0.66
0.54	-0.01 ± 0.48
0.72	0.32 ± 0.52

Table 4: α as a function of x_{D^*}. Errors are statistical only.

6 Summary and Conclusions

In conclusion, we have made preliminary measurements of the ratio $P_V = V/(V+P)$ for production of vector and pseudoscalar charmed mesons in $Z^0 \rightarrow c\bar{c}$ decay events, as well as the degree of spin alignment of D^{*+} mesons produced in inclusive Z^0 decays. Our measured value of P_V is consistent with similar measurements from LEP experiments [1, 2] and disfavors the expectation from naive spin counting. The calculations of Suzuki and Braaten, Cheung and Yuan are in rough agreement with our measured x_D-dependence of P_V . We find the degree of D^{*+} spin alignment along the flight direction, α, to be consistent with zero, in agreement with measurements at lower cm. energies. The α measurements disfavor the calculation of Suzuki.

Acknowledgments

We thank the personnel of the SLAC accelerator department and the technical staffs of our collaborating institutions for their outstanding efforts on our behalf.

References

[1] ALEPH Collab., D. Buskulic *et al.*, Z.Phys **C62** (1994) 1.

[2] DELPHI Collab., P. Abreu *et al.*, Z.Phys **C59** (1993) 533.

[3] M. Suzuki, Phys. Rev. **D33** (1986) 676.

[4] E. Braaten *et al.*, Phys. Rev. **D51** (1995) 4819,
K. Cheung and T. C. Yuan, Phys. Rev. **D50** (1994) 3181.

[5] SLD Design Report, SLAC Report 273 (1984).

[6] M. D. Hildreth *et al.*, Nucl. Inst. Meth. **A367** (1995) 111.

[7] C. J. S. Damerell *et al.*, Nucl. Inst. Meth. **A288** (1990) 288.

[8] D. Axen *et al.*, Nucl. Inst. Meth. **A328** (1993) 472.

[9] A. C. Benvenuti *et al.*, Nucl. Inst. Meth. **A290** (1990) 353.

[10] SLD Collab., K. Abe *et al.*, Phys. Rev. **D51** (1995) 962.

[11] S. Brandt *et al.*, Phys. Lett. **12** (1964) 57.
E. Farhi, Phys. Rev. Lett. **39** (1977) 1587.

[12] T. Sjöstrand and M. Bengtsson, Comp. Phys. Comm. **43** (1987) 367.

[13] G. Marchesini *et al.*, Comp. Phys. Comm. **67** (1992) 465.

[14] A full discussion of flavor tagging can be found in: SLD Collab., K. Abe *et al.*, Phys. Rev. **D53** (1996) 1023.

[15] CLEO Collab., T. Butler *et al.*, Phys. Rev. Lett. **69** (1992) 2041.

[16] Particle Data Group, Phys. Rev. **D54** (1996).

[17] CLEO Collab., Y. Kubota *et al.*, Phys. Rev. **D44** (1991) 593.

[18] HRS Collab., S. Abachi *et al.*, Phys. Lett. **B199** (1987) 585.

[19] TPC Collab., H. Aihara *et al.*, Phys. Rev. **D43** (1991) 29.

List of Authors

** K. Abe,[19] K. Abe,[29] I. Abt,[13] T. Akagi,[27] N.J. Allen,[4] W.W. Ash,[27]†
D. Aston,[27] K.G. Baird,[24] C. Baltay,[33] H.R. Band,[32] M.B. Barakat,[33]
G. Baranko,[9] O. Bardon,[15] T. Barklow,[27] A.O. Bazarko,[10] R. Ben-David,[33]
A.C. Benvenuti,[2] G.M. Bilei,[22] D. Bisello,[21] G. Blaylock,[6] J.R. Bogart,[27]
B. Bolen,[17] T. Bolton,[10] G.R. Bower,[27] J.E. Brau,[20] M. Breidenbach,[27]
W.M. Bugg,[28] D. Burke,[27] T.H. Burnett,[31] P.N. Burrows,[15] W. Busza,[15]
A. Calcaterra,[12] D.O. Caldwell,[5] D. Calloway,[27] B. Camanzi,[11] M. Carpinelli,[23]
R. Cassell,[27] R. Castaldi,[23][a] A. Castro,[21] M. Cavalli-Sforza,[6] A. Chou,[27]
E. Church,[31] H.O. Cohn,[28] J.A. Coller,[3] V. Cook,[31] R. Cotton,[4]
R.F. Cowan,[15] D.G. Coyne,[6] G. Crawford,[27] A. D'Oliveira,[7] C.J.S. Damerell,[25]
M. Daoudi,[27] R. De Sangro,[12] R. Dell'Orso,[23] P.J. Dervan,[4] M. Dima,[8]
D.N. Dong,[15] P.Y.C. Du,[28] R. Dubois,[27] B.I. Eisenstein,[13] R. Elia,[27]
E. Etzion,[4] D. Falciai,[22] C. Fan,[9] M.J. Fero,[15] R. Frey,[20] K. Furuno,[20]
T. Gillman,[25] G. Gladding,[13] S. Gonzalez,[15] G.D. Hallewell,[27] E.L. Hart,[28]
J.L. Harton,[8] A. Hasan,[4] Y. Hasegawa,[29] K. Hasuko,[29] S. J. Hedges,[3]
S.S. Hertzbach,[16] M.D. Hildreth,[27] J. Huber,[20] M.E. Huffer,[27] E.W. Hughes,[27]
H. Hwang,[20] Y. Iwasaki,[29] D.J. Jackson,[25] P. Jacques,[24] J. A. Jaros,[27]
A.S. Johnson,[3] J.R. Johnson,[32] R.A. Johnson,[7] T. Junk,[27] R. Kajikawa,[19]
M. Kalelkar,[24] H. J. Kang,[26] I. Karliner,[13] H. Kawahara,[27] H.W. Kendall,[15]
Y. D. Kim,[26] M.E. King,[27] R. King,[27] R.R. Kofler,[16] N.M. Krishna,[9]
R.S. Kroeger,[17] J.F. Labs,[27] M. Langston,[20] A. Lath,[15] J.A. Lauber,[9]
D.W.G.S. Leith,[27] V. Lia,[15] M.X. Liu,[33] X. Liu,[6] M. Loreti,[21] A. Lu,[5]
H.L. Lynch,[27] J. Ma,[31] G. Mancinelli,[22] S. Manly,[33] G. Mantovani,[22]
T.W. Markiewicz,[27] T. Maruyama,[27] H. Masuda,[27] E. Mazzucato,[11]
A.K. McKemey,[4] B.T. Meadows,[7] R. Messner,[27] P.M. Mockett,[31]
K.C. Moffeit,[27] T.B. Moore,[33] D. Muller,[27] T. Nagamine,[27] S. Narita,[29]
U. Nauenberg,[9] H. Neal,[27] M. Nussbaum,[7] Y. Ohnishi,[19] L.S. Osborne,[15]

R.S. Panvini,[30] H. Park,[20] T.J. Pavel,[27] I. Peruzzi,[12][b] M. Piccolo,[12]
L. Piemontese,[11] E. Pieroni,[23] K.T. Pitts,[20] R.J. Plano,[24] R. Prepost,[32]
C.Y. Prescott,[27] G.D. Punkar,[27] J. Quigley,[15] B.N. Ratcliff,[27] T.W. Reeves,[30]
J. Reidy,[17] P.E. Rensing,[27] L.S. Rochester,[27] P.C. Rowson,[10] J.J. Russell,[27]
O.H. Saxton,[27] T. Schalk,[6] R.H. Schindler,[27] B.A. Schumm,[14] S. Sen,[33]
V.V. Serbo,[32] M.H. Shaevitz,[10] J.T. Shank,[3] G. Shapiro,[14] D.J. Sherden,[27]
K.D. Shmakov,[28] C. Simopoulos,[27] N.B. Sinev,[20] S.R. Smith,[27] M.B. Smy,[8]
J.A. Snyder,[33] P. Stamer,[24] H. Steiner,[14] R. Steiner,[1] M.G. Strauss,[16] D. Su,[27]
F. Suekane,[29] A. Sugiyama,[19] S. Suzuki,[19] M. Swartz,[27] A. Szumilo,[31]
T. Takahashi,[27] F.E. Taylor,[15] E. Torrence,[15] A.I. Trandafir,[16] J.D. Turk,[33]
T. Usher,[27] J. Va'vra,[27] C. Vannini,[23] E. Vella,[27] J.P. Venuti,[30] R. Verdier,[15]
P.G. Verdini,[23] S.R. Wagner,[27] A.P. Waite,[27] S.J. Watts,[4] A.W. Weidemann,[28]
E.R. Weiss,[31] J.S. Whitaker,[3] S.L. White,[28] F.J. Wickens,[25] D.A. Williams,[6]
D.C. Williams,[15] S.H. Williams,[27] S. Willocq,[33] R.J. Wilson,[8]
W.J. Wisniewski,[27] M. Woods,[27] G.B. Word,[24] J. Wyss,[21] R.K. Yamamoto,[15]
J.M. Yamartino,[15] X. Yang,[20] S.J. Yellin,[5] C.C. Young,[27] H. Yuta,[29]
G. Zapalac,[32] R.W. Zdarko,[27] C. Zeitlin,[20] and J. Zhou,[20] [1]*Adelphi University, Garden City, New York 11530*

[2]*INFN Sezione di Bologna, I-40126 Bologna, Italy*

[3]*Boston University, Boston, Massachusetts 02215*

[4]*Brunel University, Uxbridge, Middlesex UB8 3PH, United Kingdom*

[5]*University of California at Santa Barbara, Santa Barbara, California 93106*

[6]*University of California at Santa Cruz, Santa Cruz, California 95064*

[7]*University of Cincinnati, Cincinnati, Ohio 45221*

[8]*Colorado State University, Fort Collins, Colorado 80523*

[9]*University of Colorado, Boulder, Colorado 80309*

[10]*Columbia University, New York, New York 10027*

[11]*INFN Sezione di Ferrara and Università di Ferrara, I-44100 Ferrara, Italy*

[12]*INFN Lab. Nazionali di Frascati, I-00044 Frascati, Italy*
[13]*University of Illinois, Urbana, Illinois 61801*
[14]*Lawrence Berkeley Laboratory, University of California, Berkeley, California 94720*
[15]*Massachusetts Institute of Technology, Cambridge, Massachusetts 02139*
[16]*University of Massachusetts, Amherst, Massachusetts 01003*
[17]*University of Mississippi, University, Mississippi 38677*
[19]*Nagoya University, Chikusa-ku, Nagoya 464 Japan*
[20]*University of Oregon, Eugene, Oregon 97403*
[21]*INFN Sezione di Padova and Università di Padova, I-35100 Padova, Italy*
[22]*INFN Sezione di Perugia and Università di Perugia, I-06100 Perugia, Italy*
[23]*INFN Sezione di Pisa and Università di Pisa, I-56100 Pisa, Italy*
[24]*Rutgers University, Piscataway, New Jersey 08855*
[25]*Rutherford Appleton Laboratory, Chilton, Didcot, Oxon OX11 0QX United Kingdom*
[26]*Sogang University, Seoul, Korea*
[27]*Stanford Linear Accelerator Center, Stanford University, Stanford, California 94309*
[28]*University of Tennessee, Knoxville, Tennessee 37996*
[29]*Tohoku University, Sendai 980 Japan*
[30]*Vanderbilt University, Nashville, Tennessee 37235*
[31]*University of Washington, Seattle, Washington 98195*
[32]*University of Wisconsin, Madison, Wisconsin 53706*
[33]*Yale University, New Haven, Connecticut 06511*
[†]*Deceased*
[a]*Also at the Università di Genova*
[b]*Also at the Università di Perugia*

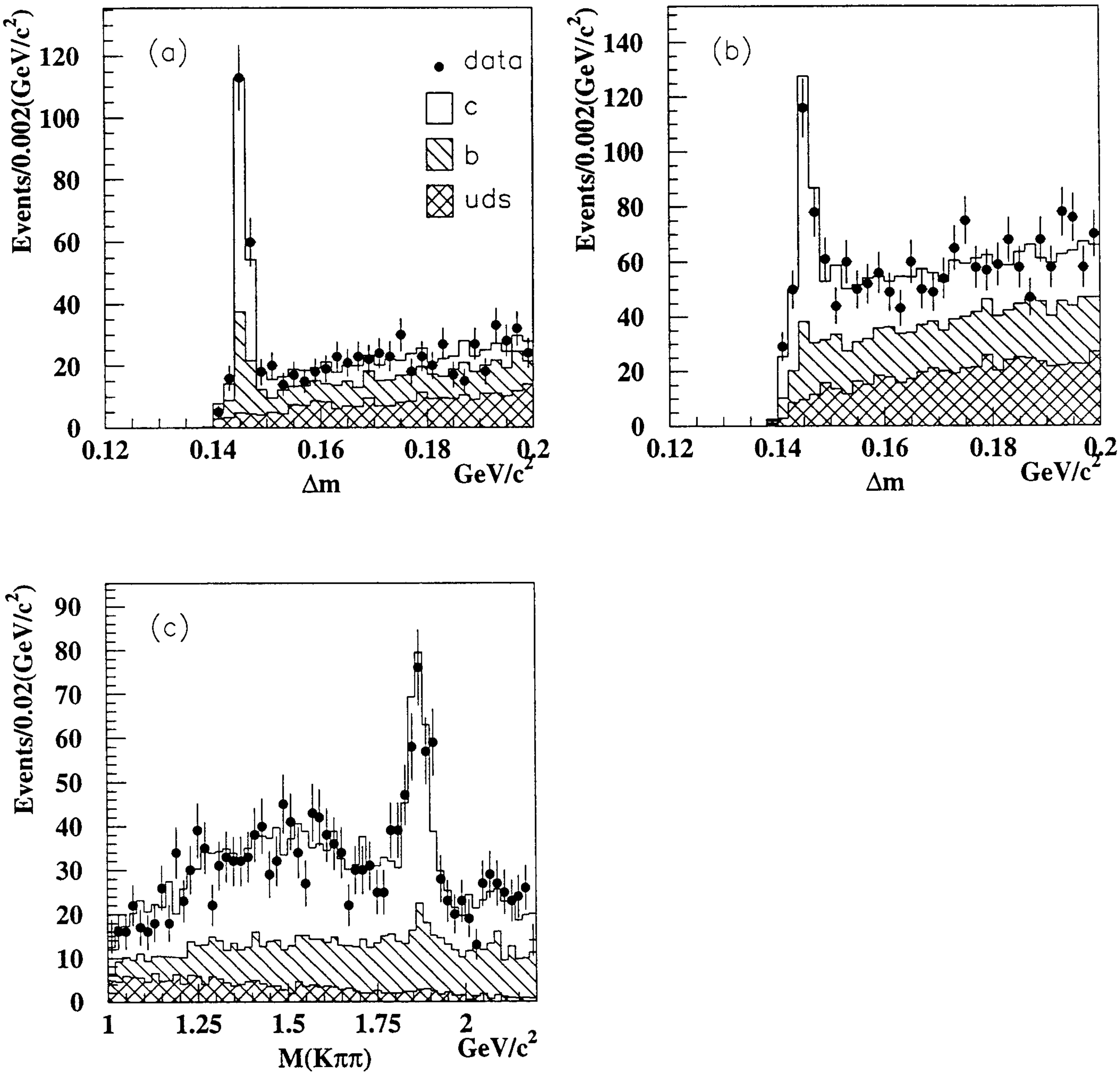

Figure 1: The Am distributions for $D^{*+} \to D^0\pi_s^+$ followed by (a) $D^0 \to K^-\pi^+$ and (b) $D^0 \to K^-\pi^+\pi^-\pi^+$, and the $M_{K\pi\pi}$ distribution for (c) $D^+ \to K^-\pi^+\pi^-$. The points represent the data and the histograms represent the Monte Carlo simulation.

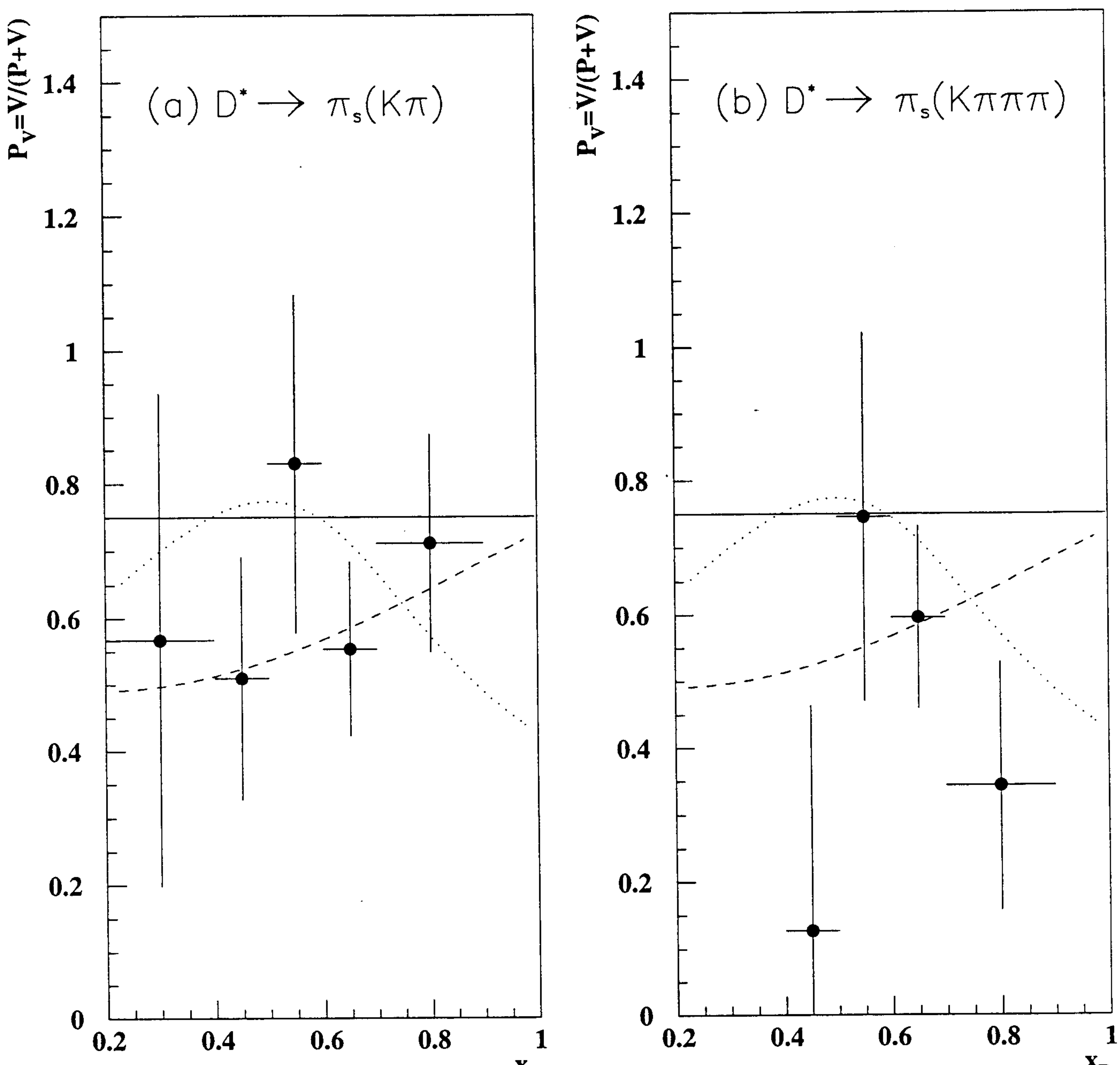

Figure 2: P_V as a function of x_D for (a) $K\pi$ and (b) $K\pi\pi\pi$ modes. The solid line represents the expectation of naive spin counting, the dotted line is the calculation by Suzuki, and the dashed line is the calculation by Braaten, Cheung and Yuan

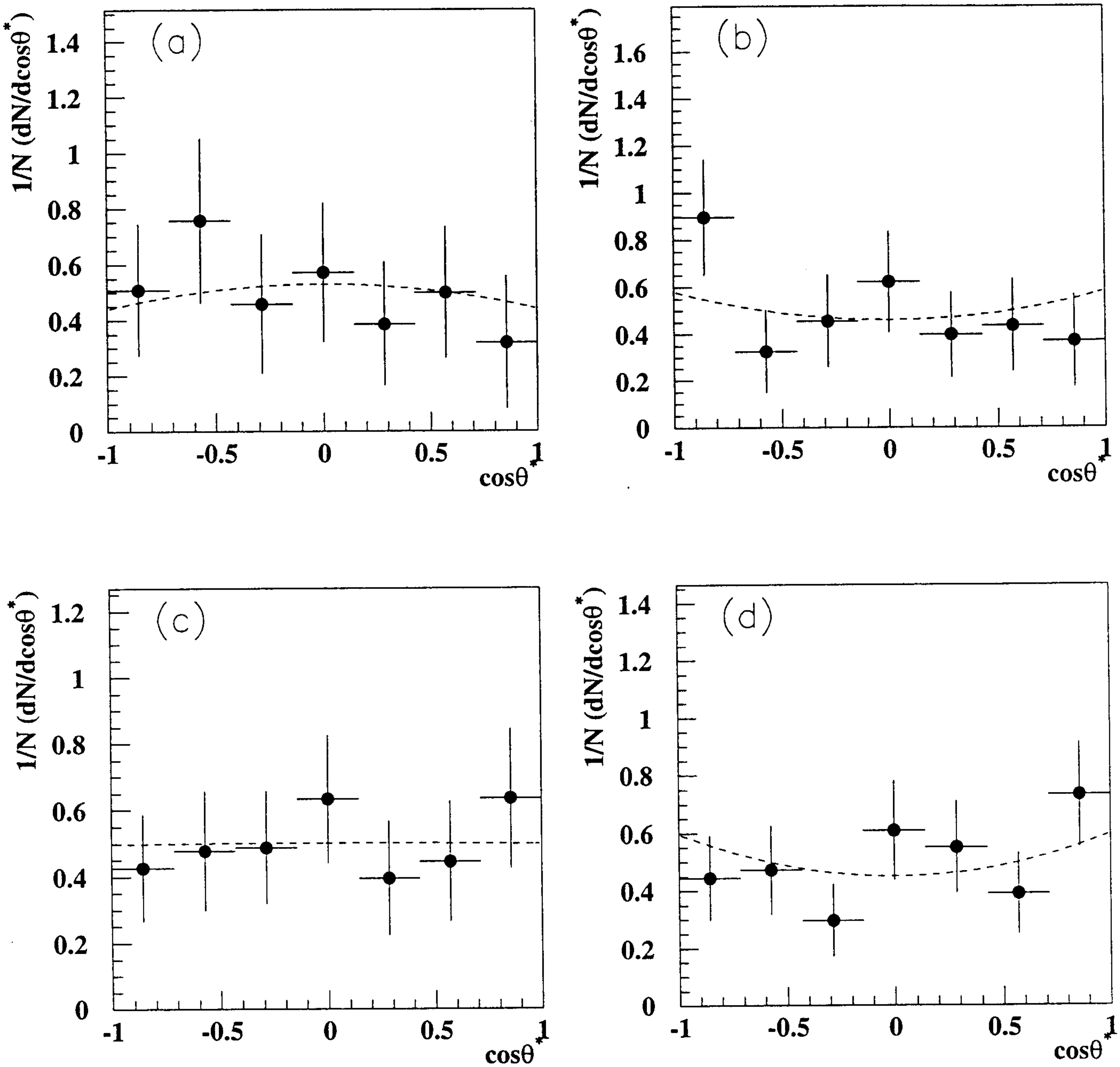

Figure 3: The $cos\theta^*$ distributions for different x_D^* bins, (a) $0.2 < x_{D^*} < 0.4$, (b) $0.4 < x_{D^*} < 0.5$, (c) $0.5 < x_{D^*} < 0.6$, and (d) $0.6 < x_{D^*} < 1.0$ with fit results shown by dashed lines. The $K\pi$ and $K\pi\pi\pi$ modes are combined in (b)-(d). For (a) only the $K\pi$ mode is shown.

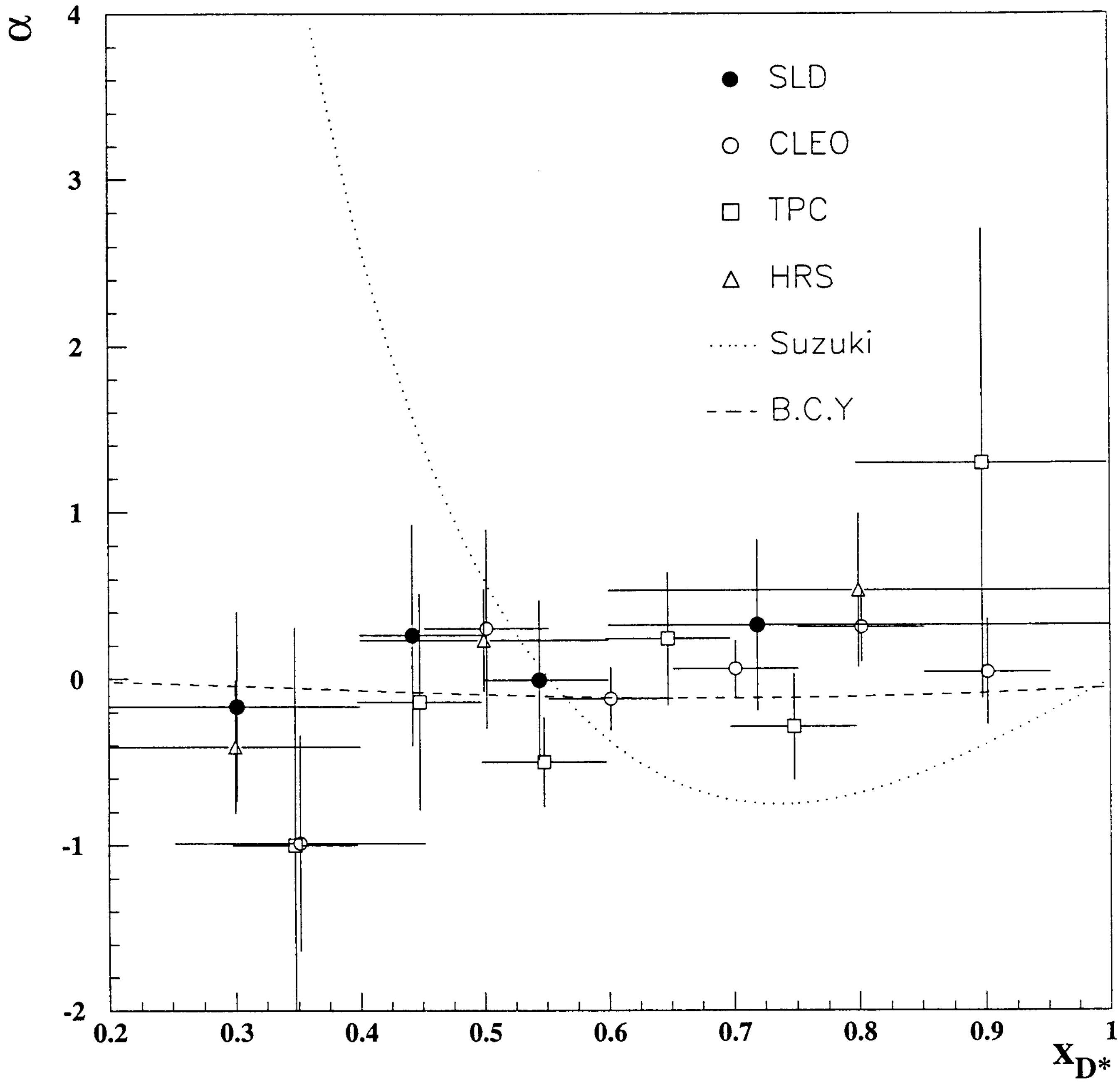

Figure 4: Fitted α as a function of x_{D^*} together with CLEO, HRS, and TPC data from lower *c.m.* energies. Model calculations are also shown (see text).